

Dickson et al., <http://www.jgp.org/cgi/content/full/jgp.201210886/DC1>

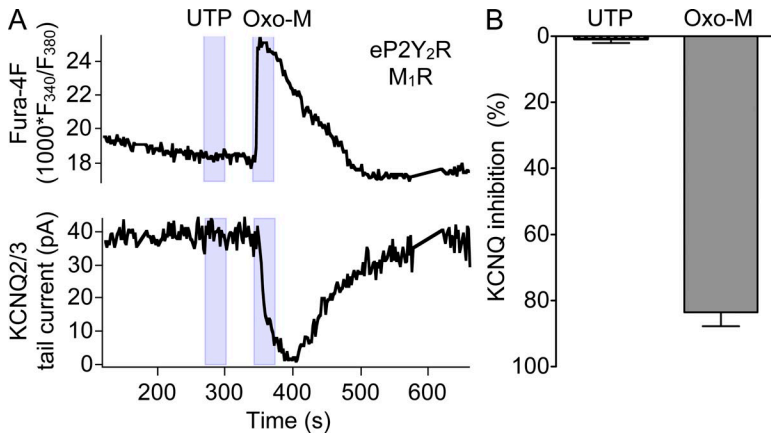


Figure S1. In whole-cell recording configuration, UTP does not elicit a calcium rise or inhibit KCNQ2/3 currents. (A) Simultaneous recording of Fura-4F (F_{340}/F_{380} ratio; top) and KCNQ2/3 tail currents (bottom) in whole-cell configuration with a patch pipette containing Fura-4F salt. Fluorescence at 340 and 380 nm was recorded by photometry. KCNQ2/3 channels were activated by a depolarization to -20 mV for 400 ms and quantified as tail currents 20 ms after repolarization to -60 mV. (B) Summary of KCNQ2/3 inhibition by $100 \mu\text{M}$ UTP ($n = 22$) and $10 \mu\text{M}$ Oxo-M ($n = 23$).

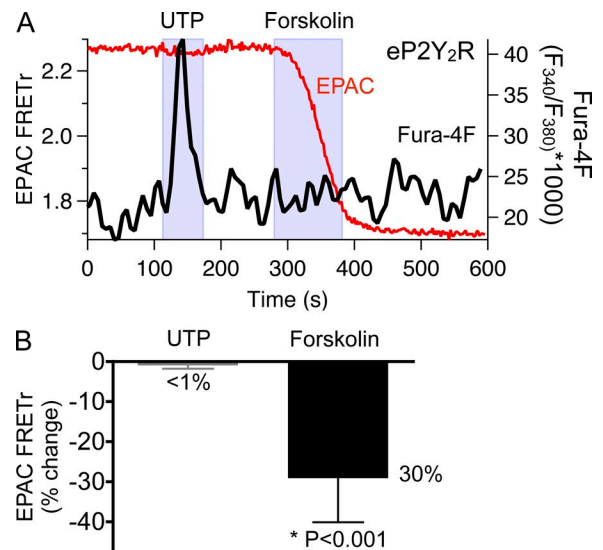


Figure S2. Endogenous P2Y receptors elevate calcium but not cAMP. (A) Simultaneous recording of FRET_r (left axis, red trace) and Fura-4F ratio (right axis, black trace) in a representative cell transfected with the cAMP reporter EPAC1. The application of $100 \mu\text{M}$ UTP leads to a change in Fura-4F ratio, reflecting a calcium rise, but no change in EPAC FRET, thus no detectable change in cAMP. Responsiveness of EPAC to cAMP is confirmed by the FRET decrease in response to $10 \mu\text{M}$ forskolin, an activator of adenylyl cyclase. (B) Summary of FRET changes in $n = 8$ experiments as in A. Significance was determined by *t* test.

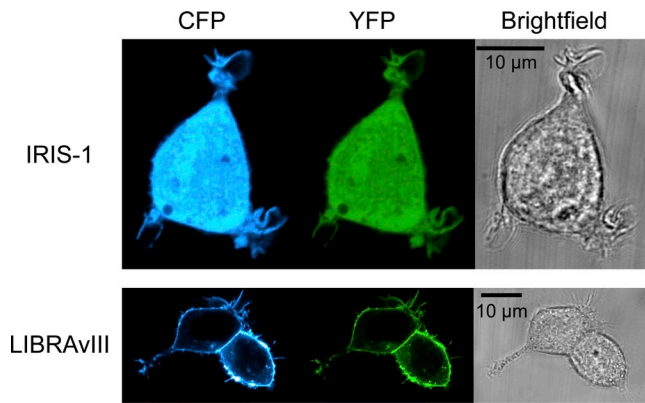


Figure S3. Expression patterns of IRIS-1 and LIBRAvIII FRET probes. Confocal images of cells transfected with the indicated plasmids (63 \times objective; 710 microscope; Carl Zeiss). The 405- and 516-nm laser lines were used for excitation of CFP and YFP. Emission was collected from 460 to 480 nm and from 540 to 580 nm. Note plasma membrane localization of LIBRAvIII and the mostly cytosolic localization of IRIS-1. The brightfield image was collected at the “transmitted” light detector with 480-nm excitation.

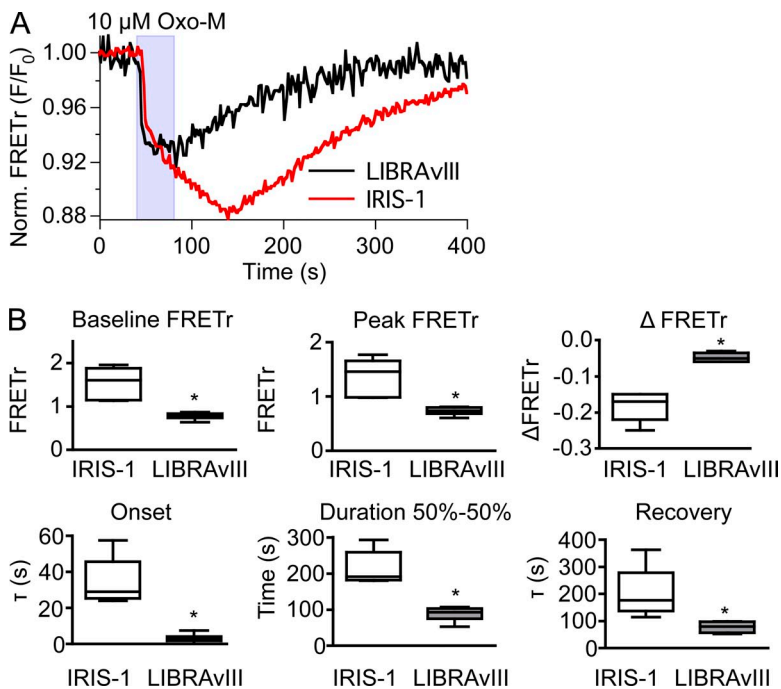


Figure S4. Comparison of the IRIS-1 and LIBRAvIII FRET probes for IP $_3$. (A) Representative responses of IRIS-1 and LIBRAvIII to 10 μ M Oxo-M. (B) Box plots comparing the mean temporal characteristics between IRIS-1 and LIBRAvIII ($n = 9$ for each probe). Box plot lines represent the mean, quartiles, and range. *, $P < 0.05$.

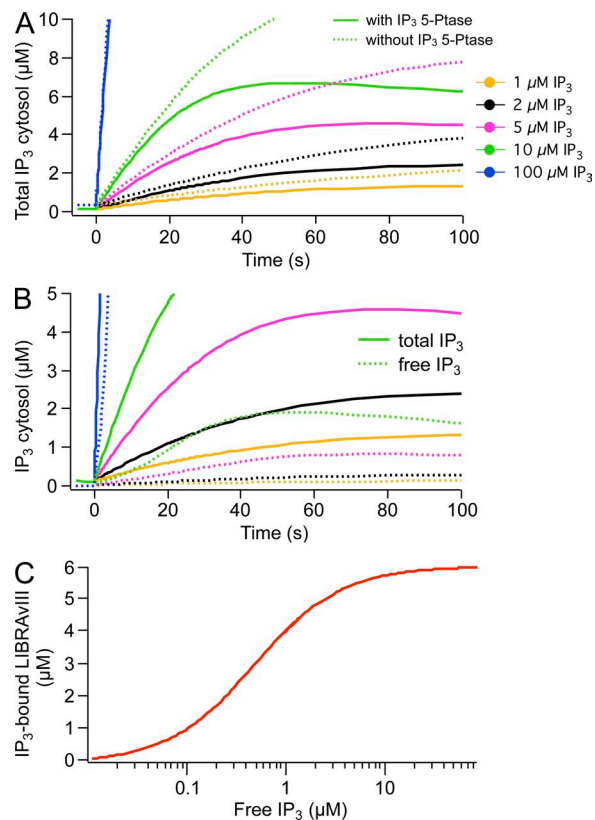


Figure S5. Model simulations of dialysis of IP₃ and response of LIBRAvIII. (A) Model outputs of total cellular IP₃ (free plus LIBRAvIII-bound) during dialysis of IP₃ from a simulated patch pipette initially filled with 100, 10, 5, 2, or 1 μM IP₃ with (solid lines) and without (dashed lines) activity of an “endogenous cytosolic IP₃ 5-phosphatase.” The rate of the phosphatase is informed by the recovery time course of the LIBRAvIII response to Oxo-M. Total LIBRAvIII concentration is 6 μM. Note that with 10 μM of initial IP₃ in the pipette, total (free plus bound) cellular IP₃ surpasses 10 μM because of buffering by LIBRAvIII. See our companion paper for details of the model. (B) Model outputs comparing free IP₃ (dashed lines) and total IP₃ (free plus LIBRAvIII-bound, solid lines) during pipette dialysis. In the simulation, “endogenous IP₃ 5-phosphatase” is active. Note that with 10 μM of initial IP₃ in the pipette, cytosolic free IP₃ does not reach 10 μM as some depletion of pipette IP₃ occurs and the 5-phosphatase is active. (C) IP₃-binding curve of LIBRAvIII extracted from the model. With a K_d of 0.5 μM, LIBRAvIII approaches saturation above 2 μM of free IP₃.

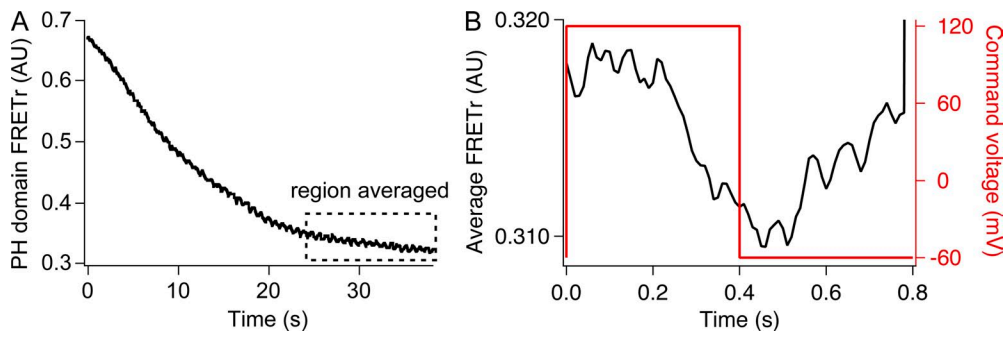


Figure S6. Time course of PIP_2 during repeated VSP activation. Cells were transfected with PH-CFP and PH-YFP (to report PIP_2 by FRET) and VSP. Cells were voltage clamped in whole-cell configuration. (A) FRET recording in response to a concatenated series of 48 depolarizations to +120 mV for 400 ms alternating with 400 ms at the -60-mV hold-

ing potential. FRET gradually decreases, indicating accumulating dephosphorylation of PIP_2 by VSP. The time course is actually sawtoothed with each depolarization. (B) FRET time course averaged cyclically for the 18 last cycles of depolarization (boxed area in A) and superimposed with the command voltage time course. The average is mildly filtered (see Materials and methods in the main text).

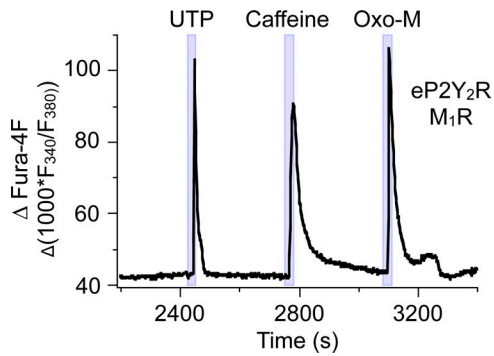


Figure S7. Evidence for ryanodine receptors in tsA cells, a calcium rise in response to caffeine. A cell transfected with M_1R loaded with Fura-4F-AM was treated with 100 μM UTP, 25 mM caffeine, and 10 μM Oxo-M during measurements by photometry. High caffeine, an activator of ryanodine receptors, increases calcium in this cell. Similar observations were made in five cells.

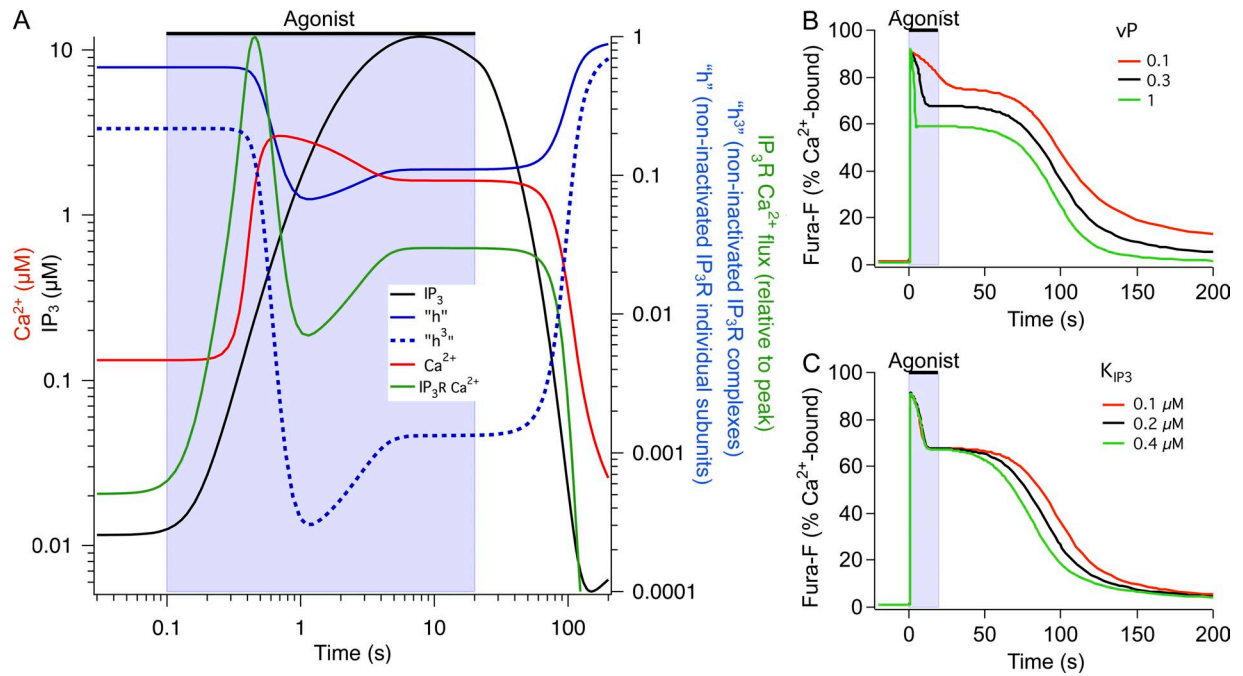


Figure S8. Origin of the plateau in the calcium and Fura-4F responses in our model. The details discussed are likely model dependent. (A) Superimposed time courses in the model of IP_3 (black), calcium (red), noninactivated IP_3R individual subunits (“h,” blue solid), noninactivated IP_3R complexes (“ h^3 ,” blue dashed), and calcium flux through IP_3Rs (green). IP_3 and calcium are plotted as absolute concentrations on the left axis, and “h,” “ h^3 ,” and scaled $IP_3R Ca^{2+}$ flux are plotted on the right axis. Note that all axes are logarithmic, a log–log plot. See main text for description. (B) Fura-4F response in the model to 10 μM Oxo-M for different values of the scaling factor of the SERCA pump (vP) showing an influence on the height of the plateau relative to the peak. This effect occurs because with faster calcium clearance, calcium has dropped more by the time the IP_3R recovers from inactivation (which is dependent on time and calcium). (C) Fura-4F response in the model to 10 μM Oxo-M for different values of the IP_3 dissociation constant of the IP_3R (K_{IP_3}), illustrating that mainly the duration of the response is affected.

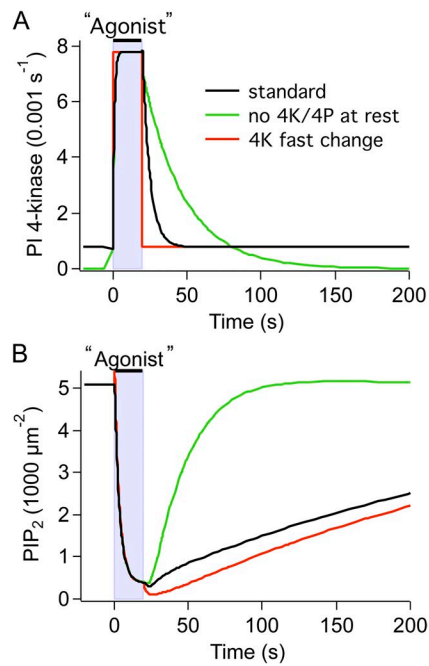


Figure S9. Establishing the time course of acceleration of PIP₂ synthesis. Computational study of the effect of the time course of the rate constant of the PI 4-kinase, k_{4k} , during 10 μM Oxo-M (A) on the time course of PIP₂ depletion (B). Almost instantaneous change of PI 4-kinase (red trace) produces a positive PIP₂ transient at Oxo-M onset and a negative PIP₂ transient at washout. Increase of k_{4k} with a time constant of 1 s or more removes the transient at onset; decrease of k_{4k} with a time constant of 10 s or more removes the transient at washout (black trace). An exponential decay of k_{4k} to zero after washout of Oxo-M with a time constant of 27.5 s produces faster PIP₂ recovery than that observed experimentally (green trace). Decay of k_{4k} with a shorter time constant produces insufficient recovery; decay of k_{4k} with a longer time constant produces overshooting recovery (both not depicted).